6468 *Inorg. Chem.* **2010**, *49*, 6468–6473
DOI: 10.1021/ic100304z

Inorganic Chemistry
Article

Sulfur-Metal Orbital Hybridization in Sulfur-Bearing Compounds Studied by X-ray Emission Spectroscopy

R. Alonso Mori,*,†,‡ E. Paris,‡ G. Giuli,‡ S. G. Eeckhout,† M. Kavčič,§ M. Žitnik,§ K. Bučar,§ L. G. M. Pettersson,∥ and P. Glatzel*,†

†*European Synchrotron Radiation Facility (ESRF), BP 220, 38043 Grenoble Cedex 9, France,* ‡*Dipartamento di Scienze della Terra, Universitá di Camerino, I-62032 Camerino, Italy,* §*J. Stefan Institute, P.O. Box 3000, SI-1001, Ljubljana, Slovenia, and* ∥*FYSIKUM, AlbaNova University Center, Stockholm University, S-10691 Stockholm, Sweden*

Received February 12, 2010

The electronic structure and ligand environment of sulfur was investigated in various sulfur-containing compounds with different structures and chemical states by using X-ray emission spectroscopy (XES). Calculations were performed using density functional theory (DFT) as implemented in the StoBe code. The sulfur chemical state and atomic environment is discussed in terms of the molecular orbitals and partial charges that are obtained from the calculations. The main spectral features can be modeled using our calculational approach. The sensitivity of the Kβ emission to the cation and the local symmetry is discussed.

Introduction

As a multivalent, nonmetallic chemical element, sulfur plays an important role in various systems. It is an essential component in biochemical systems such as amino acids, vitamins, bacteria, or proteins where iron−sulfur clusters are used for electron transfer and catalysis.[1] Natural and anthropogenic emissions of gas sulfur pollutants (H_2S, SO_2, SO_3)[2] and the acidification of surface and ground waters derived from mining activity[3] are two important examples of environmental concerns related to the presence of different forms of sulfur. Moreover, in industrial processes, such as the extraction of metals from ore deposits associated with sulfide minerals, the production of fertilizers, explosives, and cosmetics, as well as in issues around preventing poisoning of catalytic converters and in a multitude of other technological applications, sulfur has a great economic importance.[4] A deep knowledge of the sulfur ligand environment is fundamental in order to gain a more detailed understanding of the processes and reactions in which sulfur is primarily involved. Only a few in situ techniques can provide direct information on the electronic structure of sulfur, and among them, inner-shell spectroscopic methods provide the most direct and powerful means to extract information on its chemical environment. Indeed, the X-ray absorption near-edge structure (XANES) at the K-edge of S involving 1s → np transitions has been used previously to study the sulfur electronic structure of sulfur-containing minerals.[5] More specifically, the XANES pre-edge region has been identified as providing information on the amount of covalent mixing of sulfur and ligand atomic orbitals in coordination complexes of biochemical interest.[6] However, the complex XANES shape and its high sensitivity to the local structure around the sulfur atom as well as possible experimental artifacts (e.g., self-absorption in fluorescence detected XANES) may lead to difficulties in the interpretation of the XANES spectra.

The core-hole created after the ionization of the atom in the XANES process is subsequently filled by an electron from an orbital with lower binding energy. Sulfur Kβ emission spectroscopy arises from 3p to 1s electric dipole allowed transitions and, thus, directly yield the p-density of occupied

*To whom correspondence should be addressed. E-mail: glatzel@esrf.fr (P.G.), mori@esrf.fr (R.A.M.).

(1) (a) Beinert, H.; Holm, R. H.; Münk, E. *Science* **1997**, *277*, 653−9. (b) Pickering, I. J.; George, G. N.; Yu, E. Y.; Brune, D. C.; Tuschak, C.; Overmann, J.; Beatty, J. T.; Prince, R. C. *Biochemistry* **2001**, *40* (27), 8138−8145.

(2) Scaillet, B. *Science* **2008**, *319* (5870), 1628−1629.

(3) Evangelou, V. P.; Zhang, Y. L. *Crit. Rev. Environ. Sci. Technol.* **1995**, *25* (2), 141-199.

(4) (a) Niemantsverdriet, J. W. *Spectroscopy in Catalysis*, 3rd ed.; Wiley-VCH: New York, 2007. (b) Vaughan, D. J. In *Sulfide Mineral. Geochem.* **2006**, *61*, 1−5.

(5) (a) Mori, R. A.; Paris, E.; Giuli, G.; Eeckhout, S. G.; Kavcic, M.; Zitnik, M.; Bucar, K.; Pettersson, L. G. M.; Glatzel, P. *Anal. Chem.* **2009**, *81*, 6516−2525. (b) Kravtsova, A. N.; Stekhin, I. E.; Soldatov, A. V.; Liu, X.; Fleet, M. E. *Phys. Rev. B* **2004**, *69*, 13. (c) Li, D.; Bancroft, G. M.; Kasrai, M.; Fleet, M. E.; Feng, X. H.; Tan, K. *Can. Miner.* **1995**, *33*, 949−960.

(6) (a) Solomon, E. I.; Hedman, B.; Hodgson, K. O.; Dey, A.; Szilagyi, R. K. *Coord. Chem. Rev.* **2005**, *249* (1−2), 97−129. (b) Sarangi, R.; George, S. D.; Rudd, D. J.; Szilagyi, R. K.; Ribas, X.; Rovira, C.; Almeida, M.; Hodgson, K. O.; Hedman, B.; Solomon, E. I. *J. Am. Chem. Soc.* **2007**, *129* (8), 2316−2326. (c) Ray, K.; George, S. D.; Solomon, E. I.; Wieghardt, K.; Neese, F. *Chem.—Eur. J.* **2007**, *13* (10), 2783−2797. (d) Glaser, T.; Hedman, B.; Hodgson, K. O.; Solomon, E. I. *Acc. Chem. Res.* **2000**, *33* (12), 859−868.

 Published on Web 06/16/2010

valence states. Due to the electron configuration of the sulfur atom, which includes a 3p valence state, Kβ fluorescence lines reflect the chemical environment of sulfur with high sensitivity. Since the incident energy is constant and the diagram emission lines are below the absorption threshold, self-absorption effects on the spectral intensities can be neglected. Kβ emission spectroscopy has also been applied to the study of the electronic structure of sulfur in inorganic chemistry compounds.[7]

In this work, we analyze the high-resolution Kβ emission spectra of a series of sulfur-containing compounds, including various chemical states and ligand environments. The influence of these parameters on the spectral shape is analyzed by means of quantum chemical calculations based on DFT theory. The ligand environment and degree of orbital hybridization are discussed in terms of the molecular orbitals and partial charges as obtained from DFT calculations.

Experimental Section

The experiment was performed at beamline ID26 of the European Synchrotron Radiation Facility (ESRF). The beamline monochromator uses two cryogenically cooled Si crystals in (111) reflection, providing an energy resolution of 0.36 eV at the S K-edge energy (2472 eV). Higher harmonics were suppressed by two Si mirrors operating in total reflection. The incoming flux of photons, used to normalize all spectra, is monitored by the scattering from a 1 μm Silicon Nitride foil. The total flux is 5×10^{12} photons/s at 2.5 keV using the fundamental of the undulator radiation. Emission spectra were recorded by means of a high-resolution crystal spectrometer.[5a,8] The spectrometer, under vacuum conditions (10^{-6} mbar), consists of a diffraction crystal curved in Johansson geometry and a position-sensitive X-ray detector. The incident X-rays and X-ray emission angle relative to the target surface were set to 45°, giving a scattering angle of 90 degrees. Emitted photons were reflected in first order by a 3 cm high $\times$ 7.5 cm wide cylindrical Si (111) crystal (2d = 6.271 Å) with a 50 cm Rowland circle radius. The emitted photons were detected by a thermoelectrically cooled (−40 °C) charge-coupled device (CCD) detector consisting of 770 $\times$ 1152 pixels, each having a size of 22.5 $\times$ 22.5 μm^2. In order to exploit the length of the CCD camera to measure the whole Kβ spectrum simultaneously at a fixed detector position, the target was placed well inside the Rowland circle at a distance of 27 cm from the diffraction crystal. The overall experimental resolution was estimated to 0.5 eV at the energy of the S Kβ emission lines. We measured $> 10^2$ counts/s in the maximum of the Kβ spectra, and sufficient statistics were thus obtained after an acquisition time of a few minutes for each spectrum. Possible systematic errors were investigated by measurements of pure sulfur samples prepared with the same procedure and located in different positions on the sample holders, as well as repeated measurements of the reference Na_2SO_4 sample at various times during the experiment. They were found to be within the precision limit of 0.08 eV. The reference energy was set equal to 2467.15 eV for the K$\beta_{1,3}$ line of the Na_2SO_4 sample which served as a reference.[9] S Kβ emission spectra were recorded with an excitation energy of 2520 eV, assuring that resonance effects will not influence the spectra.

Table 1. Photon-Energy Values (eV) of the Maximum of the Strongest Kβ Spectral Features of Various Sulfate, Sulfite, and Sulfide Compounds

compound	formal ox. st.	Kβ'	Kβ_x	K$\beta_{1,3}$	Kβ''	Kβ_{xx}
Na_2SO_3	4+	2451.84	2463.98	2465.83	2469.60	2472.31
Na_2SO_4	6+	2452.91	2465.67	2467.15	2470.06	
$CaSO_4+H_2O$	6+	2452.69	2466.04	2466.91	2470.45	
$SrSO_4$	6+	2452.77	2465.98	2467.01	2470.37	
$BaSO_4$	6+	2452.81	2465.61	2467.18	2470.78	
$CaSO_4$	6+	2452.70	2465.98	2466.83	2470.59	
$PbSO_4$	6+	2452.79	2465.47	2467.00	2470.52	

compound	formal ox. st.	A	B	C	D
MoS_2	2−		2463.00	2464.70	2466.57
PbS	2−	2459.93		2465.69	2467.29
ZnS	2−	2458.99	2462.96	2465.89	2469.78
HgS (cinnabar)	2−	2460.39	2464.48	2466.80	2469.99
As_2S_3	2−	2459.01	2464.48	2467.16	2469.85
FeS_2	2−		2463.62	2466.22	2469.33
$Fe_{1-x}S$	2−		2462.61	2465.09	2468.16
$CuFeS_2$	2−		2463.05	2464.59	2467.34
$(Cu,Fe)_{12}Sb_4S_{13}$	2−	2459.35	2463.04	2464.71	2467.71
Cu_5Fe_4	2−		2462.60	2463.87	2467.84

The spectra were fitted with Pearson-VII functions that provide a good approximation to a Voigt profile. Four or five peaks were used for the oxy-anions and three or four for the sulfides to achieve a satisfactory fit. We note that the choice of the number of peaks to fit the experimental spectrum is arbitrary, since we do not know the exact number of electronic transitions contributing to the spectral shape, and an experimentally observed peak may be composed of several transitions that cannot be resolved experimentally.

The sulfur compounds used in this work, chosen to include different local structures, coordinations, and sulfur chemical states, are listed in Table 1. Most samples have been obtained from the mineralogical collection of the Department of Earth Sciences of the University of Camerino. All samples have been carefully characterized by X-ray diffraction to ensure the absence of multiple phases. The parameters necessary to construct the cluster models were extracted from crystallographic databases.[10] Similar samples were used elsewhere,[5a] where further details on their structure can be found.

Calculations

Ab initio quantum chemical calculations were carried out with the StoBe-deMon DFT code.[11] To model Kβ emission spectra, the Kohn−Sham orbitals of the ground state potential are used to represent both initial and final states.[12] The computed spectral transitions were convoluted with 0.5 eV FWHM Gaussian functions to model the experimental broadening. An overall shift of the energy scale was applied to each spectrum to coincide with experimental results. The exchange-correlation functionals used in the sulfur calculations were the GGA exchange functional by Becke, Be88,[13]

(7) (a) Sugiura, C.; Gohshi, Y.; Suzuki, I. *Phys. Rev. B* **1974**, *10* (2), 338−343. (b) Torres Deluigi, M.; Riveros, J. A. *Chem. Phys.* **2006**, *325* (2), 472−476. (c) Kavcic, M.; Dousse, J. C.; Szachetko, J.; Cao, W. *Nucl. Instrum. Meth., Phys. Res. Sect. B: Beam Interact. Mater. Atoms* **2007**, *260* (2), 642−646.

(8) Kavcic, M.; Karydas, A. G.; Zarkadas, C. *Nucl. Instrum. Meth., Phys. Res. Sect. B: Beam Interact. Mater. Atoms* **2004**, *222* (3−4), 601−608.

(9) Deslattes, R. D.; Kessler, E. G.; Indelicato, P.; de Billy, L.; Lindroth, E.; Anton, J. *Rev. Mod. Phys.* **2003**, *75* (1), 35−99.

(10) (a) Crystallographic and Crystallochemical Database for Mineral and their Structural Analogues. http://database.iem.ac.ru/mincryst/search.php (accessed Jun 2010). (b) Inorganic Crystal Structure Database. http://icsdweb.fiz-karlsruhe.de/ (accessed Jun 2010).

(11) StoBe-deMon (Stockholm−Berlin version of deMon, a Density Functional Theory (DFT) molecule/cluster package), version 3.0 (June 2006). http://w3.rz-berlin.mpg.de/~hermann/StoBe/ (accessed Jun 2010).

(12) Fohlisch, A.; Hasselstrom, J.; Bennich, P.; Wassdahl, N.; Karis, O.; Nilsson, A.; Triguero, L.; Nyberg, M.; Pettersson, L. G. M. *Phys. Rev. B* **2000**, *61* (23), 16229−16240.

(13) Becke, A. D. *Phys. Rev. A* **1988**, *38* (6), 3098−3100.

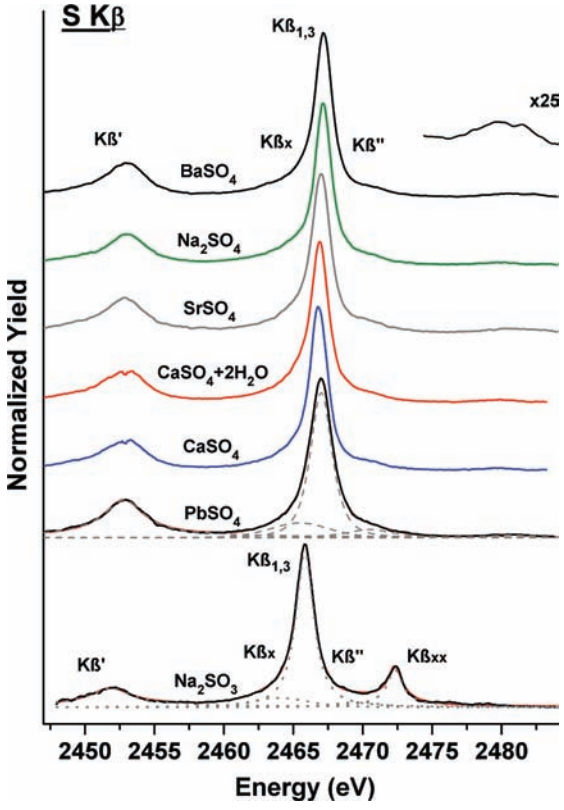

Figure 1. High resolution S Kβ X-ray spectra of some sulfate minerals and of Na_2SO_3. The spectra of $PbSO_4$ and Na_2SO_3 have been fitted with Pearson-VII functions.

and the GGA functional by Perdew, PD86,[14] for the correlation part. For further details on the calculations, see Öström et al.[15] and Triguero et al.[16] The StoBe-deMon code uses cluster models to represent extended systems. The clusters used in this work are similar to those used in Alonso Mori et al.[5a] The long-range effects of the environment in ionic systems including larger clusters makes it difficult to build a balanced neutral model, and in many cases it proved impossible to derive a computationally stable model sufficiently small to be tractable. A Mulliken analysis was performed for the discussion in terms of atomic orbitals. The results of the Mulliken analysis are shown as histograms in the figures (*vide infra*). The average of their atomic character is shown in the histograms when a spectral feature is composed of various molecular orbitals with similar character.

Results and Discussion

The analysis of the results is separated into oxidized (sulfate and sulfite) and reduced (sulfides) sulfur species. The assignment of the spectral features in previous works is presented and critically discussed in light of the data of the present work that were obtained with improved instrumental resolution and compared with new quantum chemical calculations.

A. Oxidized Sulfur (S^{6+} and S^{4+}). S Kβ emission spectra of various sulfate, and one sulfite, compounds are shown in Figure 1. The emission energies of the maxima for the main spectral features, labeled Kβ', Kβ_1, Kβ_x, and Kβ'' as well as Kβ_{xx} for the sulfite, are reported in Table 1. The spectra have already been described by several authors.[7b,17] We observe a previously unreported feature in the sulfates around 2480 eV (see magnified spectrum in Figure 1), which we assume is due to multielectron excitations. The spectrum of Na_2SO_3 is similar to those of the sulfates, except for the additional feature Kβ_{xx} at higher energies (Figure 1). The feature Kβ'' (2469.60 eV) in the sodium sulfite spectrum has not been previously reported (Table 1).

Previous works show calculations based on LCAO molecular orbital approaches, which inferred the valence molecular orbital structure of the sulfate $(SO_4)^{2-}$ [18] and sulfite $(SO_3)^{2-}$ [18b,c,e] ions, and can be used to discuss the Kβ emission spectra. The sulfur and oxygen valence orbital electrons combine following the symmetry of the compound, T_d for the sulfate ion and the lower C_{3v} symmetry for the sulfite ion, to form molecular orbitals. According to the mentioned LCAO calculations, the sulfate ion has seven occupied molecular orbitals in the valence level, labeled according to the irreducible representations of T_d, with symmetries $1a_1$, $1t_2$, $2a_1$, $2t_2$, 1e, $3t_2$, and $1t_1$[19] in order of increasing energy. By the dipole selection rule, transitions into the 1s level are allowed only from the orbitals of t_2 symmetry. Thus, the presence of three spectral peaks, Kβ', K$\beta_{1,3}$, and Kβ'', can be explained as transitions from the molecular $1t_2$ (mainly composed of S3p + O2s), $2t_2$ (mainly S3p + O2p), and $3t_2$ (mainly S3d + O2p) orbitals, respectively. The Kβ_x feature, however, cannot be explained within this approach. The previous calculations similarly give for the sulfite ion a valence structure consisting of the following occupied molecular orbitals: $1a_1$, 1e, $2a_1$, 2e, $3a_1$, 3e, 4e, $1a_2$, and $4a_1$.[20] Dipole transitions into the 1s shell are allowed from the molecular orbitals with a_1 and e symmetry. The sulfite experimental spectral features are therefore assigned to all aforementioned valence orbitals except $1a_2$. On the basis of their energies, the first peak, Kβ', is due to 1e with a small contribution of $1a_1$ (mainly populated by S3p and O2s). The main peak, K$\beta_{1,3}$, is assigned to 2e and $3a_1$ (mainly S3p + O2p). The shoulder, Kβ_x, at lower energy is associated with $2a_1$ (mainly S3p and O2s 2p). Finally, the feature Kβ_{xx} has been denoted in the literature as Kβ'' and ascribed to the $4a_1$ orbital (mainly O2p and little S3p).[20] The higher instrumental resolution in the present study leads to a reassignment of Kβ'' to the feature at 2469.60 eV, reported here for the first time, and to which we ascribe the $4a_1$ orbital, whereas the origin of Kβ_{xx} cannot be explained within the LCAO approach.

(14) (a) Perdew, J. P., Correction. *Phys. Rev. B* **1986**, *34* (10), 7406−7406. (b) Perdew, J. P. *Phys. Rev. B* **1986**, *33* (12), 8822−8824.
(15) Ostrom, H.; Fohlisch, A.; Nyberg, M.; Weinelt, M.; Heske, C.; Pettersson, L. G. M.; Nilsson, A., *Surf. Sci.* **2004**, *559* (2−3), 85−99.
(16) Triguero, L.; Pettersson, L. G. M.; Agren, H. *J. Phys. Chem. A* **1998**, *102* (52), 10599−10607.
(17) (a) Torres Deluigi, M.; Perino, E.; Olsina, R.; Riveros de la Vega, A. *Spectrochim. Acta, Part. B* **2003**, *58* (9), 1699−1707. (b) Sugiura, C. *J. Phys. Soc. Jpn.* **1995**, *64* (10), 3840−3852. (c) Taniguchi, K. *Bull. Chem. Soc. Jpn.* **1984**, *57* (4), 915−920.
(18) (a) Bishop, D. M. *Theor. Chim. Acta* **1967**, *8* (4), 285. (b) Manne, R. *J. Chem. Phys.* **1967**, *46* (12), 4645. (c) Prins, R. *J. Chem. Phys.* **1974**, *61* (7), 2580−2591. (d) Johansen, H. *Theor. Chim. Acta* **1974**, *32* (3), 273−278. (e) Uda, E.; Kawai, J.; Uda, M. *Phys. Res. Sect. B: Beam Interact. Mater. Atoms* **1993**, *75* (1−4), 24−27.
(19) Adachi, H.; Taniguchi, K. *J. Phys. Soc. Jpn.* **1980**, *49*(5), 1944–1953.
(20) (a) Karlsson, G.; Manne, R. *Phys. Scr.* **1971**, *4* (3), 119. (b) Mogi, M.; Ota, A.; Ebihara, S.; Tachibana, M.; Uda, M. *Nucl. Instrum. Meth., Phys. Res. Sect. B: Beam Interact. Mater: Atoms* **1993**, *75* (1−4), 20−23.

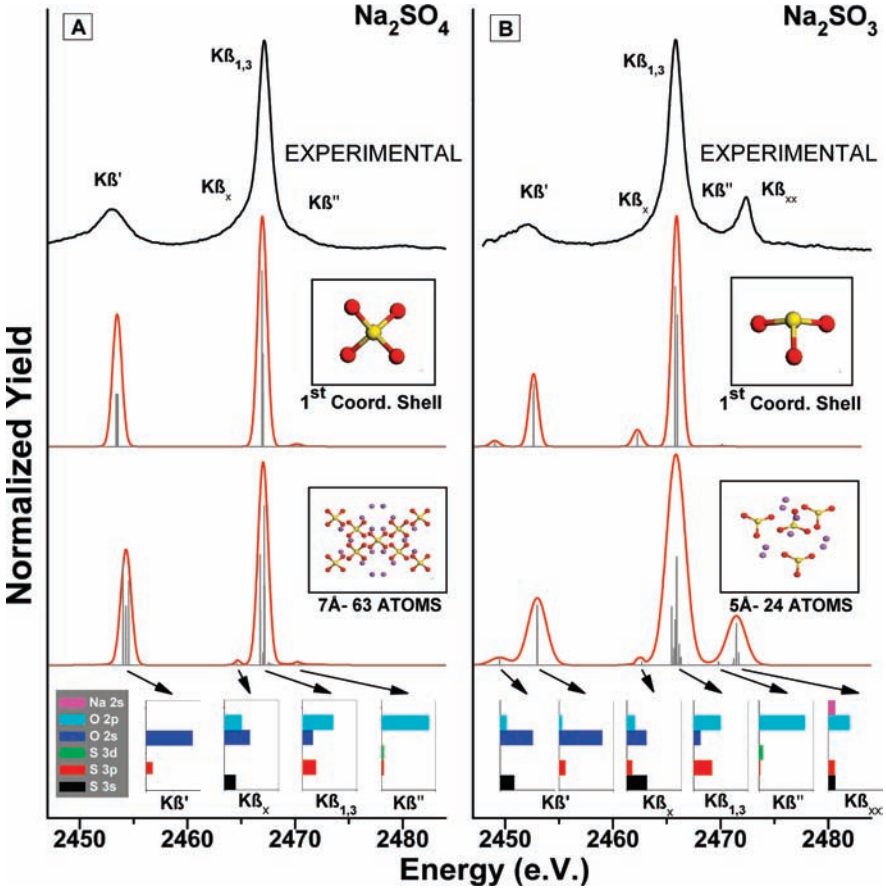

Figure 2. S Kβ X-ray experimental spectra of sodium sulfate and sodium sulfite along with calculations with different cluster sizes. A scheme of the atomic contributions to the transitions that give rise to spectral features is shown in the bottom.

Ground state DFT calculations were used in the present study for modeling the experimental spectra.[12] In Figure 2A, we show the theoretical spectrum for Na_2SO_4 including the first coordination sphere for sulfur, i.e., the tetrahedral sulfate ion, $(SO_4)^{2-}$. The calculation is in good agreement with the experimental spectrum, indicating that the cations do not significantly influence the spectral profile. The spectral features can be assigned to molecular orbitals following a Mulliken analysis. The character of the molecular orbitals contributing to the sulfate spectral features is shown in Table 2. We note that the intensity of peak Kβ_x is underestimated in the calculations. The reason is that, for the spectrum shown, only the anion, i.e., a small five-atom $(SO_4)^{2-}$ cluster with T_d symmetry, was used in the calculations. However, a larger cluster including the cations changes the point group symmetry, and as a consequence a different mixing of the atomic orbitals will be allowed, leading to a new configuration of molecular orbitals with different dipole transition matrix elements that form the Kβ spectrum. We can observe this effect in the calculation including a larger 7 Å Na_2SO_4 cluster shown in Figure 2A, where the Kβ_x feature is better reproduced. Moreover, in the calculation of the $(SO_3)^{2-}$ cluster (Figure 2B), the Kβ_x feature is also visible due to its lower C_{3v} symmetry. In the larger Na_2SO_4 calculation, additional symmetry-allowed transitions model the Kβ spectrum. The results of the atomic orbital population analysis are similar to those of the sulfate ion calculation. A scheme of the atomic contributions to the molecular orbitals associated with the transitions producing the different spectral features obtained by the 7 Å Na_2SO_4 cluster calculation is shown in the bottom of Figure 2A.

Table 2. Character of the Molecular Orbitals Contributing to the Spectral Features for Sulfate, Sulfite and Sulfide Clusters

features	$(SO_4)^{2-}$	$(SO_3)^{2-}$			ZnS	
		2449.47 eV	2458.97 eV			
Kβ'	S3p 12% O2s 86%	S3s 26% O2s 60% and O2p12%	S3p 12% O2s 80% O2p 6%	A	Zn3d 99% S3p 1%	
Kβ_x	S3s 21% O2s 47% O2p 32%	S3s 37% S3p 10% O2s 36% O2p 15%		B	central S3p 6% other S3p 43% Zn4s 33% Zn3p 8%	
K$\beta_{1,3}$	S3p 25% O2s 19% O2p 56%	S3p 42−26% O2s 8−18% O2p ∼50%		C	central S3p 30% other S3p 43% Zn3p 19%	
Kβ''	S3p 4% S3d 8% O2p 88%	S3p1−3% S3d 8−5% O2p ∼85%		D	central S3p 8% other S3p 80% Zn4s 4% Zn3p 4%	
		Only for Na_2SO_3 cluster				
Kβ_{xx}		S3s 13% S3p ∼12% O2p ∼40% Na2s ∼13%				

Similar DFT calculations were performed for sodium sulfite (Figure 2B). The atomic partial charges modeling the spectral shape obtained with the four atoms anion $(SO_3)^{2-}$ are reported in Table 2. The calculation underestimates the

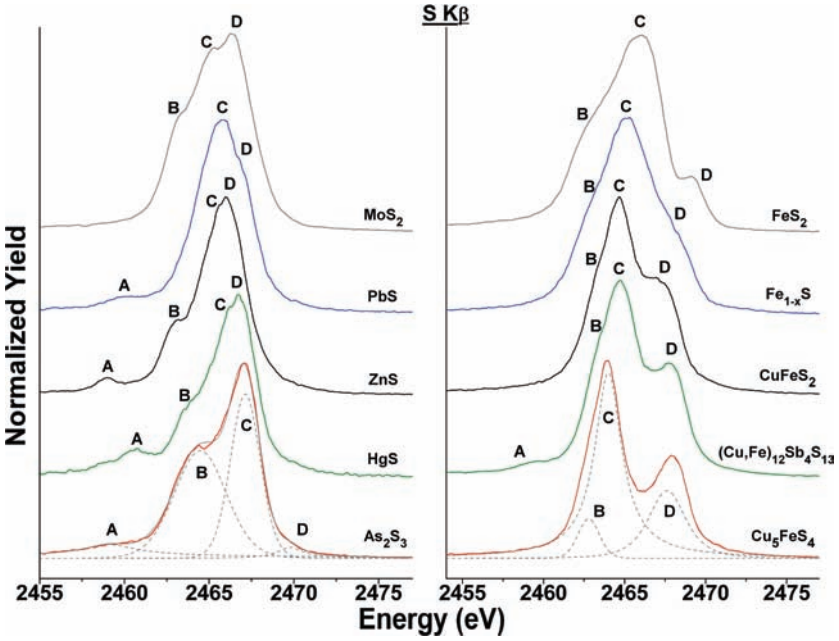

Figure 3. High-resolution S Kβ X-ray spectra of various sulfide compounds where the spectra of As_2S_3 and Cu_5FeS_4 have been fitted with Pearson-VII functions.

strength of the transition moments between the orbitals associated with Kβ''. The character of this peak, similar to the Kβ'' feature in the sulfate spectrum, supports the assignment of this peak, which was not previously reported in the literature, as Kβ''. Accordingly, we label the feature present at higher energies (2472.3 eV) as Kβ_{xx}, which was reported in other works as Kβ''. Kβ_{xx} is not reproduced in the simulation based on the naked anion, but in the calculation with a larger 5 Å Na_2SO_3 cluster this feature is clearly visible (Figure 2B). Symmetry arguments similar to those used for the feature Kβ_x in the sulfate discussion can be invoked here for the feature Kβ_{xx}, which is associated with transitions that are only allowed in the lower (C_3) symmetry of the 5 Å Na_2SO_3 calculation. These examples demonstrate the importance of symmetry arguments to account for spectroscopic data. According to the larger simulation, Kβ_{xx} is the only feature where sodium cations contribute to the spectral shape, and therefore Kβ_{xx} would be a spectral feature that can be expected to be sensitive to changes related to the cations in oxy-anions. However, the spectral intensity mainly arises from O and S, and the sensitivity to the type of cation may be weak. All other spectral features simulated with the larger cluster are in good agreement with the simple four-atom naked anion calculation.

A remarkable difference between both sulfate and sulfite species is the shape of Kβ', which is characteristic of oxy-anions reflecting the binding between the S3p and O2s orbitals. Kβ' is broader in the sulfites where two molecular orbitals with different electronic character are involved, whereas in the sulfates the low-energy transitions are forbidden (Table 2). Besides, feature Kβ_{xx} is not present in the sulfate spectra and can thus be used to identify the presence of tetravalent sulfur in unknown or multivalent systems. We also note that a S 3d contribution is only weakly found in Kβ'' for sulfur

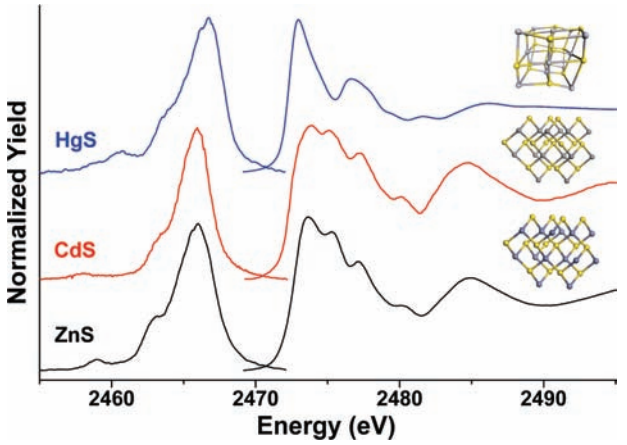

Figure 4. S K-edge XANES and Kβ emission spectra of α-HgS (cinnabar), CdS (hawleyite), and ZnS (sphalerite). The atomic structures are also shown.

oxy-anions, although it has been discussed earlier in the literature.[21]

B. Reduced Sulfur (S^{2-}). Sulfur Kβ emission spectra of various sulfide compounds are reported in Figure 3. The spectral shape is strongly affected by the structure, bond distances, angles, and ligand type. The energy values of the characteristic peaks obtained from the fits are given in Table 1. The majority of the sulfur Kβ emission spectra shown here have been reported previously by Sugiura et al.,[7a,22] although with considerably lower instrumental resolution.

The five Cu/Fe containing sulfide spectra ($CuFeS_2$, $(Cu,Fe)_{12}Sb_4S_{13}$, Cu_5FeS_4, $Fe_{1-x}S$, and FeS_2) have similar spectral shapes, indicating a similar p-electron density in the valence level of S. They are characterized by a prominent peak, C; a well-resolved feature at higher energy, D; and a shoulder at lower energy, B. The spectrum of $(Cu,Fe)_{12}Sb_4S_{13}$

(21) Stromberg, A.; Wahlgren, U.; Pettersson, L. G. M.; Siegbahn, P. E. M. *Chem. Phys.* **1984**, *89*, 323−328.

(22) Sugiura, C.; Suzuki, I.; Kashiwakura, J.; Gohshi, Y. *J. Phys. Soc. Jpn.* **1976**, *40* (6), 1720−1724.

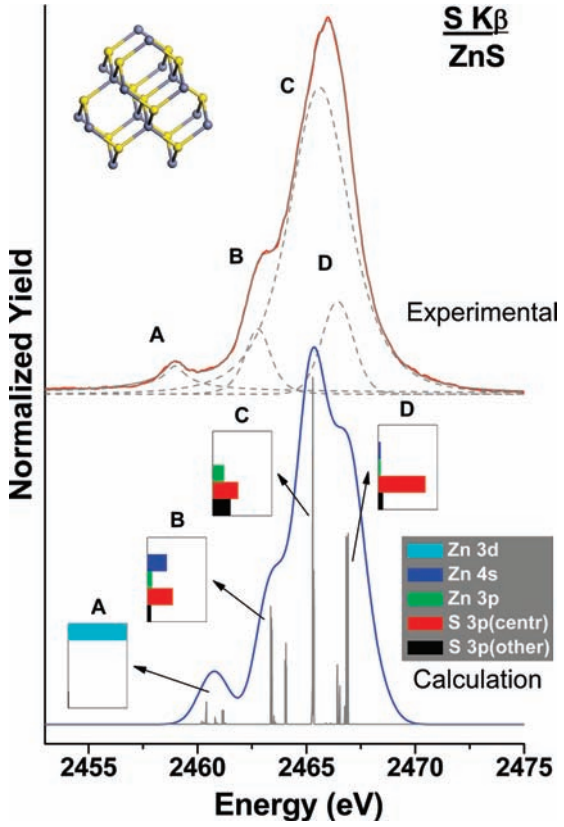

Figure 5. S Kβ X-ray experimental spectra of ZnS along with a 4.5 Å cluster theoretical spectrum. Schemes show the atomic contributions to the transitions modeling the spectra.

also shows a clear feature, labeled A, at even lower energy that is not observed in the other Cu/Fe sulfides. We did not achieve convergence in the DFT calculations for these systems, and an analysis of the spectra based on the molecular orbital transitions is thus not possible.

The metal cations in ZnS, CdS, and α-HgS exhibit a filled highest d shell (Zn $3d^{10}$, Cd $4d^{10}$, and Hg $5d^{10}$), and sulfur is expected to have a similar valence electronic structure for the three systems.[5a] This leads to very similar Kβ XES spectra even for different sulfur local structures and coordinations. As shown in Figure 4, the S local symmetry is T_d in ZnS and CdS and distorted O_h in the case of α-HgS. The emission spectra consist of two features around 2466 eV (C and D), a shoulder in the low energy side (B) and a third feature at even lower energy (A). A comparison between Kβ XES and XANES nicely illustrates the sensitivity of the different techniques (Figure 4). While the three Kβ XES spectra show a very similar shape, in XANES this only holds for ZnS and CdS, whereas the α-HgS XANES spectral shape is very different from that of the other two compounds. The reason is that Kβ probes localized occupied orbitals that participate in the bonding, which is similar in the three systems with filled d-shell cations, while the XANES spectral shape depends on the scattering properties of the extended atomic environment.

We have modeled the experimental S Kβ emission spectrum of ZnS by means of DFT calculations. The theoretical and experimental spectra are in good agreement (cf. Figure 5). The simulated cluster includes 4.5 Å and 29 atoms. The character of the molecular orbitals involved in the transitions associated with the spectrum is reported in Table 1. The feature A is due to the transition into the 1s shell from a group of molecular orbitals with almost pure Zn d character. The d orbitals in the metal cation of these compounds are fully occupied and barely mix with the sulfur orbitals. The character of the rest of the molecular orbitals indicates some hybridization between the central and the neighboring sulfur atoms.

The results obtained for ZnS can be extrapolated to α-HgS and CdS. Similarities with the spectra of As_2S_3 and PbS, where the feature A is visible, can also be found; these metal cations also have a filled d-orbital shell close to the valence shells. Moreover feature A is also present in the only Cu/Fe sulfide experimental spectrum with a full d-orbital provided by the Sb atoms, $(Cu,Fe)_{12}Sb_4S_{13}$. We assume that this feature is related to a full d-orbital close to, or in, the valence shells.

Conclusions

The comparison of S Kβ XES spectroscopy and theoretically calculated spectra is a valuable tool to extract information about the electronic structure of sulfur in various sulfur-containing compounds. The calculations, based on DFT, provide the contributions of the different molecular orbitals to the spectral shape, giving information about the bonding and hybridization of sulfur with the cations. The localized character of the orbitals involved in the emission process renders the DFT cluster simulations an appropriate approach, where the main spectral features can be reproduced and thus interpreted in terms of transitions between molecular orbitals

The Kβ spectra are also influenced by the sulfur local symmetry that determines the intensity of the electron transitions to the S 1s orbital. The spectral shape for all sulfur oxyanions is similar. However, an additional feature at high energies appears in the sulfite spectra due to the lower symmetry. Calculations of the sulfides based on DFT are challenging, and convergence was achieved only for ZnS with a filled 3d shell.

A more in-depth interpretation of the Kβ spectral shape is currently limited by the accuracy of the computational approach. The results obtained on sulfates and sulfites in the present study are promising. A more suitable approach for the sulfides may be band-structure calculations that consider the long-range order. XES may be more accessible to theoretical modeling than XANES due to the localized character of the orbitals that give rise to the spectra, while the two techniques are complementary in the information they can provide. Unlike for XAS measurements, no monochromatic tunable incident energy is required, and an efficient XES spectrometer can push the detection limit into the range of a few hundred parts per million.

Acknowledgment. This work was supported by the European Synchrotron Radiation Facility (ESRF). The authors thank the ID26 staff and the ESRF support groups for technical assistance.